Electronic Supporting Information (ESI) for

Synthesis of monodisperse water-stable surface Pb-rich $CsPbCl_3$ nanocrystals for efficient photocatalytic CO_2 reduction

Jingrun Zhu,[a] Yihua Zhu,*[a] Jianfei Huang,[c] Lu Hou,[a] Jianhua Shen,[a] and Chunzhong Li*[ab]

a Key Laboratory for Ultrafine Materials of Ministry of Education; Shanghai Engineering Research Center of Hierarchical Nanomaterials; School of Materials Science and Engineering, East China University of Science and Technology, Shanghai 200237, China.

b School of Chemical Engineering, East China University of Science and Technology, Shanghai 200237, China.

c Center for Polymers and Organic Solids, Department of Chemistry and Biochemistry University of California, Santa Barbara CA 93106, USA.

Experimental procedures

Materials

Lead chloride (99.99 %, Adamas), Cesium acetate (99.9%, 3AChemicals), Manganese chloride (99.99%, Aladdin), Nickel (II) chloride anhydrous (99%, Apollo), n-Hexane (99.99 %, Aladdin), Oleyl amine (90 %, OAm, Innochem), Oleic acid (90 %, OA, innochem), 1-Octadecene (90%, ODE, Aldrich). All reagents were used as received without further purification.

Preparation of surface Pb-rich perovskite NCs

$CsPbCl_3$ NCs were synthesized using a previously reported method by a slight modification.[1-4] The cesium precursor (0.105 M) was synthesized by mixing cesium acetate, OA, and ODE at 90 °C and kept at room temperature (25 °C) under N_2 environment. The lead precursor was prepared by mixing dried and degassed 0.1232 g $PbCl_2$, 1.6 mL OA, and 1.6 mL OAm in 15 mL ODE at 110 °C under N_2 atmosphere. The lead solution was heated up to 180 °C followed by quick injection of the cesium precursor (1.2 mL). After a few seconds, the reaction was ended by water bath. The synthesized $CsPbCl_3$ NCs were centrifuged at 10000 r.p.m. for 5 minutes. The precipitation was redispersed in n-hexane and stored at room temperatue in dark for further experiments. Similarly, doped $CsPbCl_3$ NCs were prepared by tuning the contents of Ni^{2+}, Mn^{2+}, and Ca^{2+} ions in lead precursor. In this study, the contents of impurity ions are twice times than Pb^{2+} in mixture solution. 5 mL synthesized NCs in n-hexane were centrifuged at 10000 r.p.m. for 10 minutes. After removing supernatant, the precipitation was dried at room temperature under vacuum conditions. The amount of soild QDs is about 0.12 g after vacuum conditions. Then 5 mL of deionized water were carefully added for liquid-solid interpenetration under room temperature. After more than 12 hours under static state, the precipitation was treated by ultrasonic to disperse NCs in water. Then solution was filtered (220 nm) for further tests.

The samples to be treated by LSI method should be dense QDs solid layers formed after centrifugation (10000 rpm, 5 min). The key step in the experimental

process is to ensure that the samples remain dense and stacked before adding deionized water. At the beginning, only the samples at the liquid-solid interface are eroded by water. The eroding boundary will move down in the QDs solid layer, with time going by.

Photochemical reactions for CO_2 reduction

It should be noted that all samples were measured without sacrificial donors. The photochemical reactions for CO_2 reduction were conducted under a solid-gas mode in a 280 mL sealed Pyrex bottle filled with CO_2 and H_2O vapor. The glass fiber films were roasted in a muffle furnace at 800 °C. 6 mg photocatalysts were loaded on the prepared glass fiber films. The sample films and 500 μL deionized water were put into the Pyrex bottle. Then the bottle was repeatedly degassed and filled with CO_2 to remove air. A 300 W Xe lamp (PLS-SXE300D, Perfectlight company) with a standard AM 1.5G filter was used as the solar light source. The intensity of light source was calibrated to 150 mW cm^{-2} by a light irradiation meter (FZ400, Newport. Co.) The product was analyzed by gas chromatograph (GC2060, Valco Instruments Co., Inc.) equipped with a thermal conductivity detector (TCD) and a flame ionization detector (FID) in series.

Characterization

The high-resolution transmission electron microscope (HR-TEM) images were obtained with a JEM-2100F TEM operated at an accelerating voltage of 200 kV. The high-angle annular dark-field scanning transmission electron microscopy (HAADF-STEM) experiments were carried out using a FEI Talos microscope operated at 200 kV. X-ray photoelectron spectroscopy (XPS) measurements were recorded on a Thermo Fisher ESCALAB 250 Xi spectrometer. Inductively coupled plasma mass spectrometer (ICP-MS) measurements were carried on NexION 2000-(A-10). Powder X-ray diffraction (XRD) patterns were collected on a Rigaku Corporation max 2550 VB Rotating Anode X-ray Powder Diffractometer with Cu Kα radiation (λ = 1.54060 Å). Room-temperature X-band electron paramagnetic resonance (EPR) spectra were recorded at a microwave frequency of 9.4 GHz on a Bruker ELEXSYSII E500 spectrometer. The samples were prepared by dropping solutions on quartz substrates.

Fourier transform infrared (FRIT) spectrometer spectra in the region of 400 - 4000 cm^{-1} were recorded on a Thermo Fisher Scientific Nicolet 6700 Spectrometer.

The absorption spectra were recorded on a Perkin Elmer Lambda 950 UV/Vis Spectrophotometer. In a routine measurement, the colloidal perovskite quantum dots were kept in quartz cuvettes and the spectra were measured from 300-800 nm. Photoluminescence and photoluminescence excitation spectra were obtained by using a Shimadzu RF-6000. Photoluminescence decays were measured on a time-resolved single photon counting using a Hamamatsu C11367-32 Quantaurus-Tau spectrometer in solvent mode at room temperature.

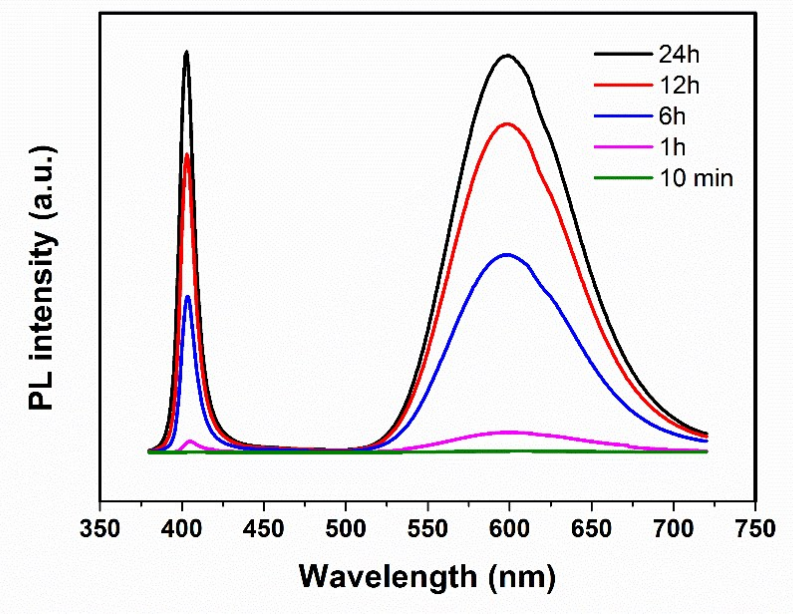

Fig. S1 PL spectra of Mn-doped $CsPbCl_3$ QDs with different post-synthetic time.

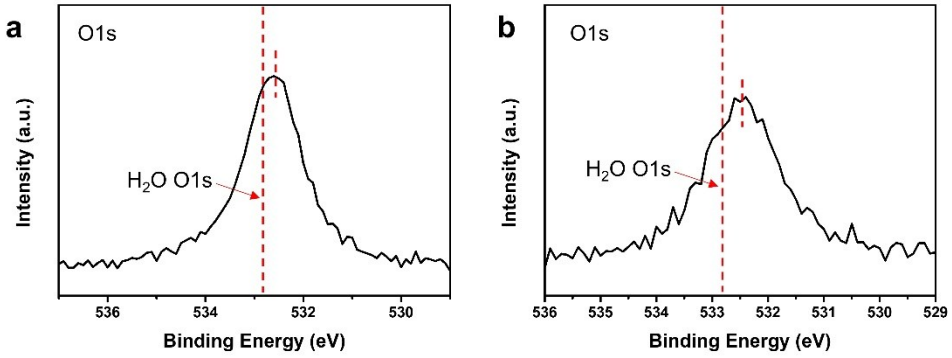

Fig. S2 XPS of the O 1s core level of (a) Ni and (b) Mn-doped surface Pb-rich $CsPbCl_3$ NCs.

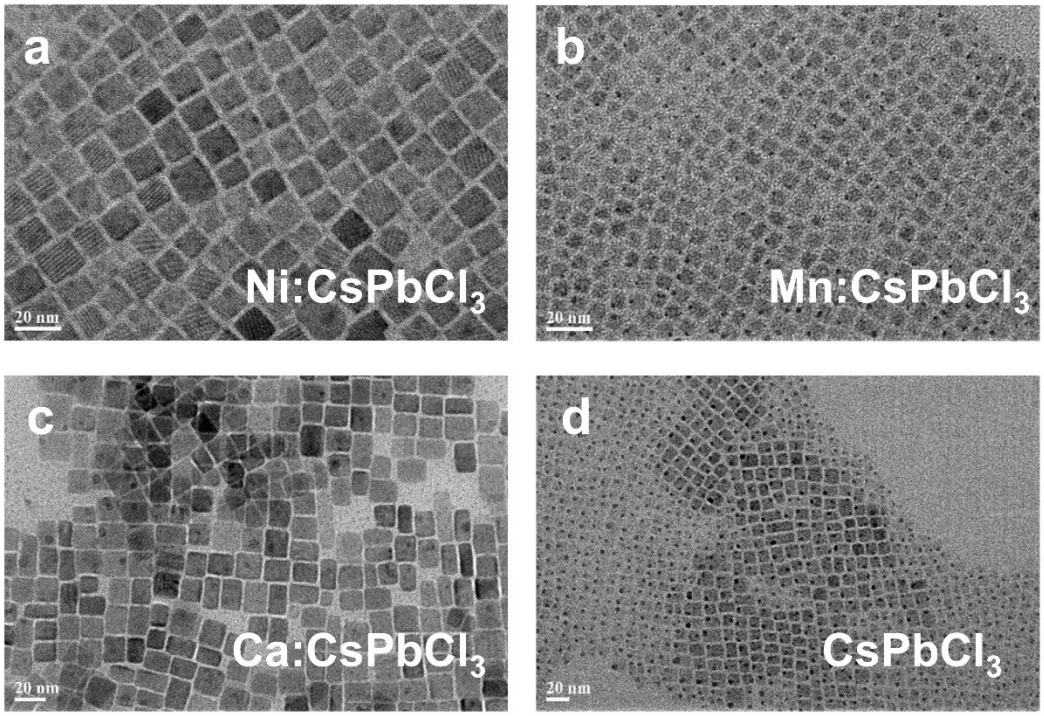

Fig. S3 TEM images of Ni (a), Mn (b), Ca (c) doped $CsPbCl_3$ NCs and undoped $CsPbCl_3$ NCs (d).

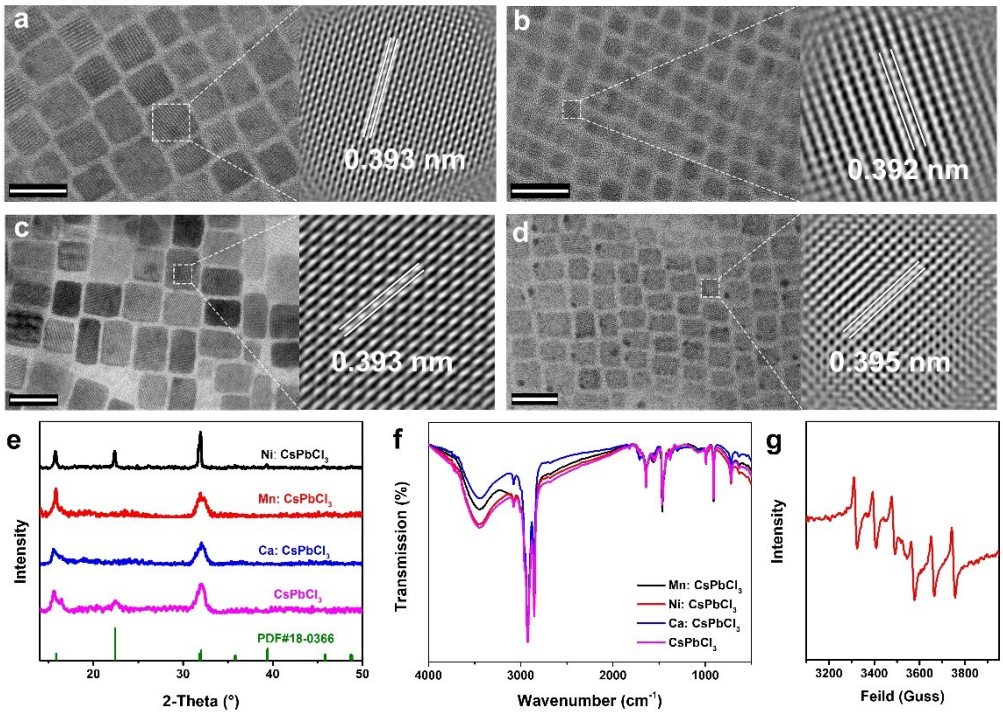

Fig S4. TEM and FFT-filtered HRTEM images of Ni-doped $CsPbCl_3$ NCs (a), Mn-doped $CsPbCl_3$ NCs (b), Ca-doped $CsPbCl_3$ NCs (c), and $CsPbCl_3$ NCs (d). Scale bar is 20 nm in each image. (e) XRD patterns of doped and undoped $CsPbCl_3$ NCs. (f) FTIR spectra of doped and undoped $CsPbCl_3$ NCs. (g) Room-temperature X-band EPR spectrum of Mn-doped $CsPbCl_3$ QDs.

The broad bands in the range of 3420-3444 cm^{-1} can be assigned to the O-H stretching vibration arising from the COOH of oleic acid (OA). The small peaks at 3081 cm^{-1} are due to the C-H stretching vibration modes of C-H arising from the C=C-H bonds of OA and oleyl amine (OAm). The bands at 2921 and 2853 cm^{-1} can be assigned to C-H asymmetric (υ_{as}) and symmetric (υ_s) stretching vibration of methylene (CH_2) groups in the alkyl chain of OA and OAm. The peaks at ~1641 cm^{-1} can be assigned to the N-H bending vibration of OAm. The peaks at 720 cm^{-1} can be attributed to the N-H out-of-plane deformation vibration of OAm.

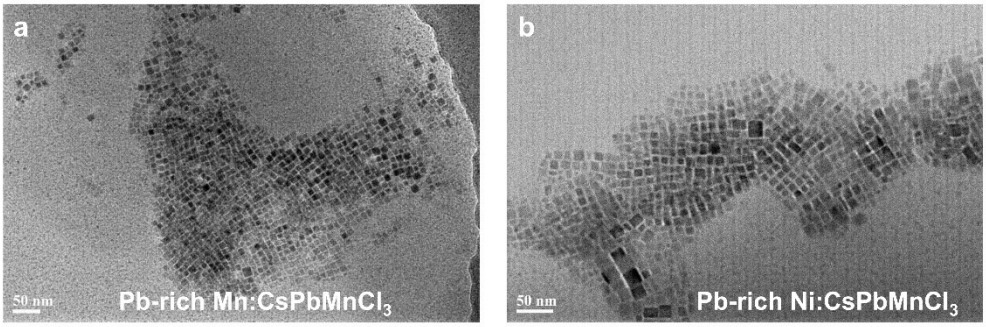

Fig. S5 TEM images of Pb-rich Mn-doped $CsPbCl_3$ NCs (a) and Pb-rich Ni-doped $CsPbCl_3$ NCs (b).

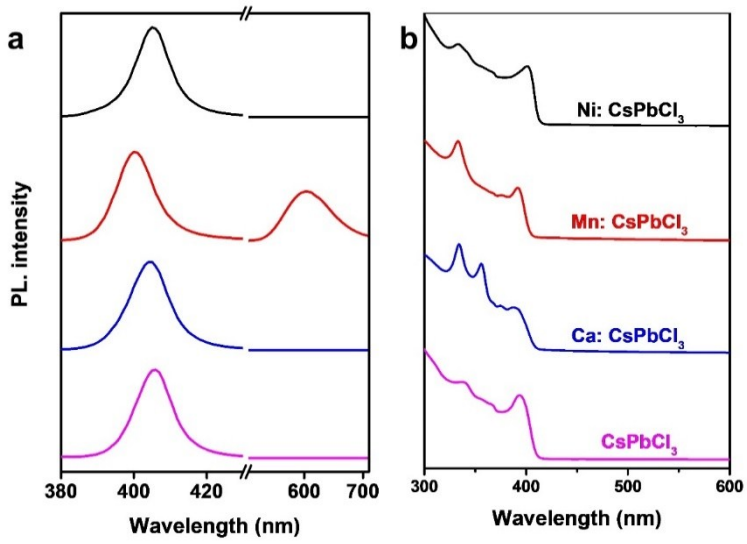

Fig. S6 The PL spectra (a) and absorption spectra (b) of doped and undoped cesium lead chloride perovskite QDs.

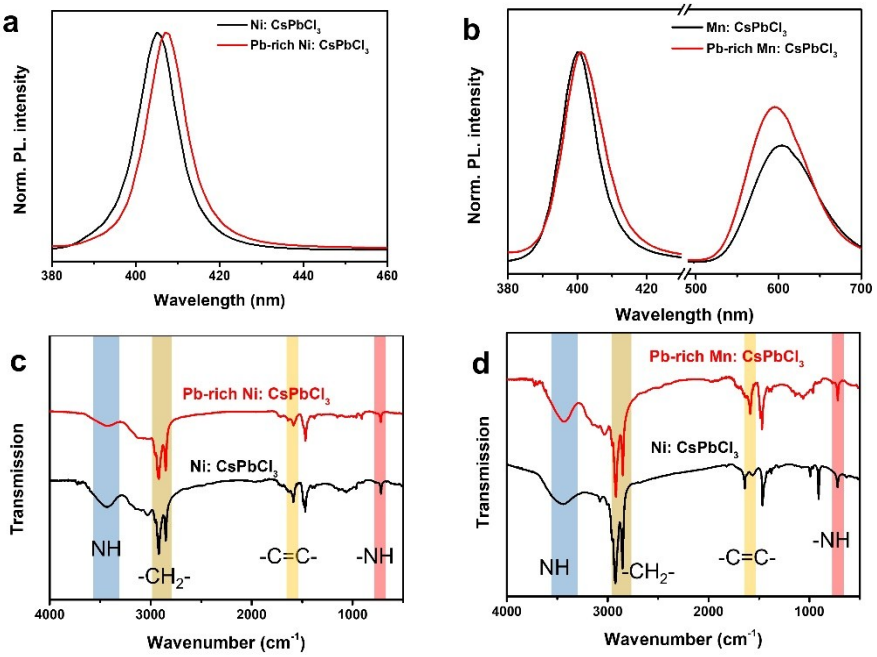

Fig. S7 FTIR spectra of Ni-doped (a) and Mn-doped (b) $CsPbCl_3$ QDs. PL spectra of Ni-doped (c) and Mn-doped (d) $CsPbCl_3$ QDs.

The PL intensity ratios of Mn to $CsPbCl_3$ host exhibit impressively increase. In order to investigate the shifted values, we compare the PL spectra of Mn-doped $CsPbCl_3$ with different concentration in n-hexane solution. The intensity both of Mn^{2+} ions and $CsPbCl_3$ host emission increase first and then decrease with the concentrations increasing, implying the self-filtering effect of QDs. The concentration-dependent data of Mn-to-$CsPbCl_3$ PL intensity ratios can be well fitted by a Hill equation. The equation is as following:

$$v = 5.13372 \times \frac{c^{-0.6484}}{21.2371 + c^{-0.6484}} \quad (1)$$

where v is the value of Mn-to-$CsPbCl_3$ PL intensity ratios; c is the concentration of colloidal $CsPbCl_3$ QDs with Mn doping.

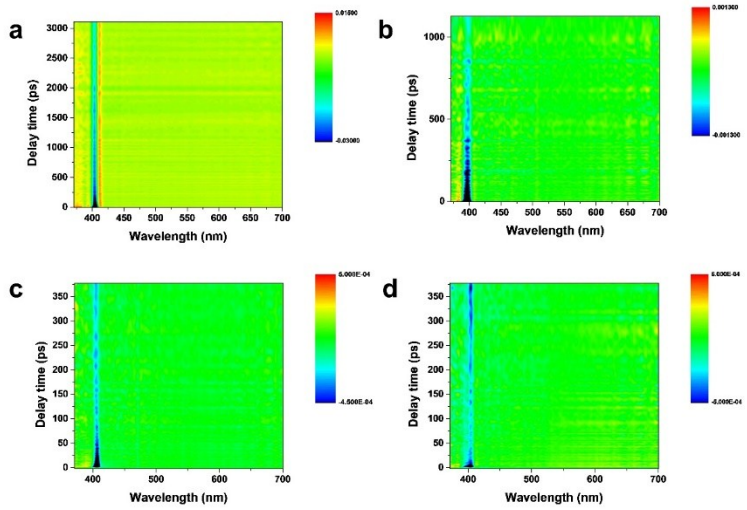

Fig. S8 The transient absorption spectra of Ni-doped $CsPbCl_3$ QDs in Hexane (a) and Pb-rich Ni-doped $CsPbCl_3$ QDs in water (c). The transient absorption spectra of Mn-doped $CsPbCl_3$ QDs in n-hexane (b) and Pb-rich Mn-doped $CsPbCl_3$ QDs in water (d).

Generally, the TA spectrum shows a negative absorption feature, the ground state bleaching (GSB) signals, which is centered close to the average band gap energy. Obviously, the red shifts of GSB signals indicate the decrease of the optical band gap after the LSI process.

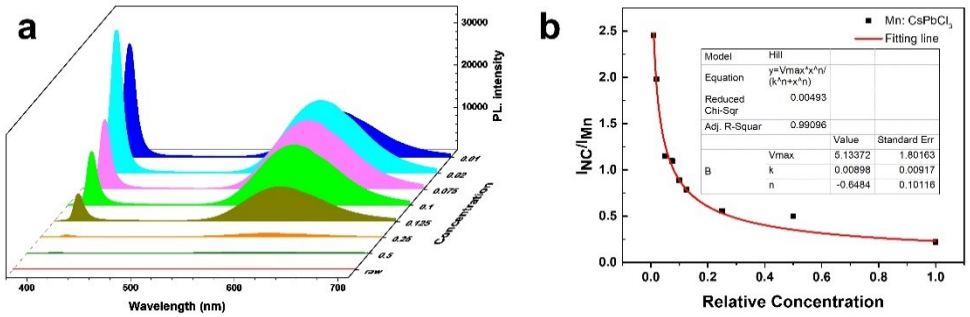

Fig. S9 (a) Concentration-dependent PL spectra of Mn-doped $CsPbCl_3$ QDs in n-hexane. (b) Concentration-dependent plots of the intensity ratios of Mn-to-$CsPbCl_3$ host NCs.

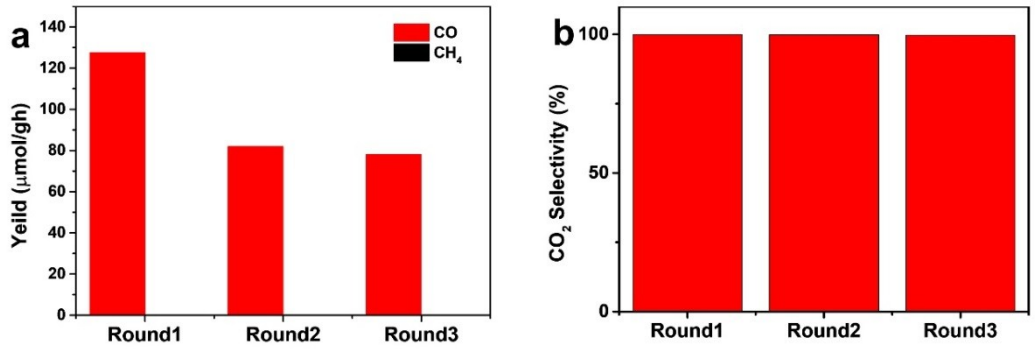

Fig. S10 (a) CO generation of surface Pb-rich Mn-doped $CsPbCl_3$ NCs for three consecutive runs of 2 h each. (b) CO_2 selectivity of surface Pb-rich Mn-doped $CsPbCl_3$ NCs for three consecutive runs of 2 h each.

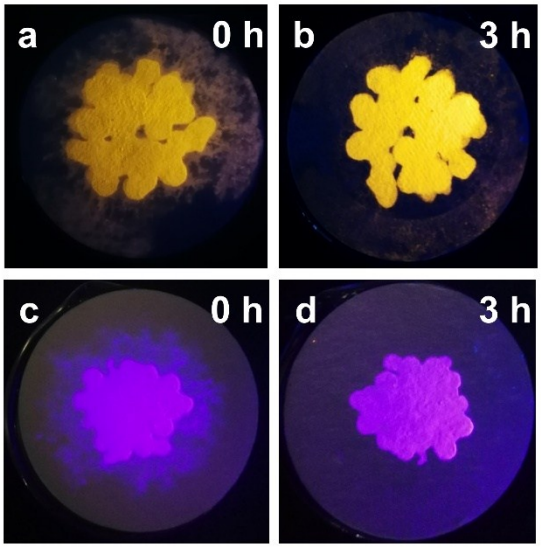

Fig. S11 Digital photos of surface Pb-rich Mn-doped $CsPbCl_3$ NCs before (a) and after (b) photoreduction reaction. Digital photos of surface Pb-rich Ni-doped $CsPbCl_3$ NCs before (c) and after (d) photoreduction reaction.

Table S1 Molar ratios of Cs to Pb measured by XPS.

Sample	$CsPbNiCl_3$	Pb-rich $CsPbNiCl_3$	$CsPbMnCl_3$	Pb-rich $CsPbMnCl_3$
Ratio of Cs / Pb	1:1.5	1:11.5	1: 1.3	1:42.5

Table S2 Molar concentrations of divalent cation cations substitution measured by ICP-MS.

Sample	Mn (at %)	Ni (at %)	Ca (at %)	Pb (at %)
$CsPbMnCl_3$	42.1	-	-	57.9
$CsPbNiCl_3$	-	3.3	-	96.4
$CsPbCaCl_3$	-	-	19.6	80.4

Table S3 Summary of halide perovskite QD-based photosystems for CO_2 reduction.

Sample	Light source	Products	Yield (μmol/gh)	Reference
$CsPbBr_3$/GO	100 W Xe lamp (150 mW cm^{-2})	CO, CH_4, H_2	23.7	5
$CsPbBr_3$ NCs	300 W Xe lamp (100 mW cm^{-2})	CO, CH_4, H_2	4.3	6
$CsPbBr_3$/g-C_3N_4	300 W Xe lamp (λ > 420 nm)	CO, CH_4	149	7
$CsPbBr_3$/TiO_2	150 W Xe lamp (λ > 420 nm)	CO, CH_4, H_2	2.29	8
Surface Pb-rich Ni: $CsPbCl_3$ NCs	300 W Xe lamp (150 mW cm^{-2})	CO, CH_4	169.37	This work

References

1. A. Pan, B. He, X. Fan, Z. Liu, J. J. Urban, A. P. Alivisatos, L. He and Y. Liu, ACS Nano 2016,10, 7943-7954.
2. W. Liu, Q. Lin, H. Li, K. Wu, I. Robel, J. M. Pietryga, V. I. Klimov, J. Am. Chem. Soc. 2016, 138, 14954-14961.
3. Z. J. Yong, S. Q. Guo, J. P. Ma, J. Y. Zhang, Z. Y. Li, Y. M. Chen, B. B. Zhang, Y. Zhou, J. Shu, J. L. Gu, L. R. Zheng, O. M. Bakr and H. T. Sun, J. Am. Chem. Soc., 2018, 140, 9942-9951.
4. J. K. Chen, J.P. Ma, S. Q. Guo, Y. M. Chen, Q. Zhao, B. Zhang, Z. Li, Y. Zhou, J. S. Hou, Y. Kuroiwa, C. Moriyoshi, O. M. Bakr, J. Y. Zhang, and H. Sun, Chem. Mater. 2019, 31, 3974-3983.
5. Y. F. Xu, M. Z. Yang, B. X. Chen, X. D. Wang, H. Y. Chen, D. B. Kuang and C. Y. Su, J. Am. Chem. Soc. 2017, 139, 5660-5663.
6. J. Hou, S. Cao, Y. Wu, Z. Gao, F. Liang, Y. Sun, Z. Lin and L. Sun, Chem. Eur. J. 2017, 23, 9481-9485.
7. M. Ou, W. Tu, S. Yin, W. Xing, S. Wu, H. Wang, S. Wan, Q. Zhong and R. Xu, Angew. Chem. Int. Ed. 2018, 57, 13570-13574.
8. Z. Kong, J. Liao, Y. Dong, Y. Xu, H. Chen, D. Kuang and C. Su, ACS Energy Lett. 2018, 3, 2656-2662.